

# FLUID-STRUCTURE INTERACTION (FSI) MODELLING OF SOLAR PANEL INSTALLATIONS IN BUILDINGS FOR TYPHOON RESILIENCE

Conrad Allan Jay Pantua<sup>1,2\*</sup>, John Kaiser Calautit<sup>1</sup>, Yupeng Wu<sup>1</sup>

<sup>1</sup> Department of Architecture and Built Environment  
University of Nottingham, Nottingham NG7 2RD, UK

<sup>2</sup> Mechanical Engineering department,  
De La Salle University, Manila, Philippines

## ABSTRACT

Current renewable energy mounting technologies with its different installation methods, and mounting locations are consequently affected by wind loads differently. Using the FSI approach, this study evaluated solar panels attached to the gabled roof of a single detached low-rise building. The building was subjected to typhoon strength winds in an urban environment using Computational Fluid Dynamics (CFD) analysis. A typhoon's Atmospheric Boundary Layer (ABL) flow simulation was conducted to predict the pressure coefficient distribution around the structure. A validated structural model of the support attached to the roof was then developed, and the analysis performed using FSI to predict deflections, stress concentration areas and potential failure in the structural supports and attachments. The results of the study showed the weaknesses in the current design considering the roof shape, pitch, structural support, arrangements and materials. Results show areas of failure in the panels with regards to wind angle direction and installation location.

**Keywords:** Typhoon, Computational Fluid Dynamics; Finite element analysis, Fluid structure interaction, Urban environment, Buildings

## NOMENCLATURE

Abbreviations	
ABL	Atmospheric Boundary Layer

CAD	Computer Aided design
CFD	Computational fluid dynamics
FEA	Finite element analysis
FSI	Fluid structure interaction
GGI	General Grid Interface
LES	Large Eddy Simulations
OSB	Oriented Strand Board
RANS	Reynolds-averaged Navier-stokes equations
SPF	Spruce Pine form
TKE	Turbulent Kinetic energy
<i>Symbols</i>	
$U$	velocity magnitude (m/s)
$\alpha$	power law coefficient

## 1. INTRODUCTION

Last 2013, the Philippines made headlines as it was hit by Typhoon Haiyan which was the strongest storm ever recorded at landfall. The super typhoon had sustained wind speeds up to 315 kilometres per hour (195 mph) and gustiness up to 380 kilometres per hour (235 mph) [1]. The damage to infrastructure and casualties were staggering. A total of 6,300 people died in the aftermath with 28,000 injuries [2]. Around 1.1 million homes were damaged or destroyed with an economic impact of 12.9 billion USD [3]. A visual evaluation and survey of the damage along Typhoon

Haiyan’s path in Tacloban and East Guian, Philippines showed that 53% of low rise detached buildings suffered wind damage and the most critical damage is roof system failure which accounted for 21% of all damage [4]. Immediately after the disaster there was interest and clamour for better typhoon resilient buildings in the country [5]. Unfortunately, very few researches were conducted on typhoon resilient infrastructure in the Philippines [6]. Most of the studies were concentrated on the effect of hurricanes to low rise structures in the United States. On the other hand, current solar panel mounting technologies are also affected by wind loads. Solar panel installations may increase the uplift forces and over estimation of these forces can increase the cost of construction costs. The present structural codes require further information for it to be directly applicable to the solar systems. Lastly, limited studies were conducted to look at the overall wind loads brought to the building with solar panels installed [7]. Majority of the studies are on the estimation of the wind loads on the panels itself and not on the overall effect on the entire building after panel installation. There is a clear need to evaluate the current solar panel arrangements and configurations and its structural integrity to prevent or minimise damage in future climactic events. This research proposes the use of fluid-structure interaction (FSI) method for the analysis of wind pressures on a low-rise gabled timber buildings under typhoon strength wind conditions to assess the structural response of its components, sheathing panels and solar panel arrangements.

The FSI analysis for the gabled roof building model is performed using the commercial program ANSYS 18.1 which includes the CFD FLUENT, Structural Mechanical and System Coupling tools. The developed model is utilised to investigate the stresses, strains and displacements on the frame and sheathing of a low-rise gabled building made of timber at different wind angles. This method is also utilised to determine the wind loading effect of solar panels attached to a gabled roof at different wind angles and speeds.

## 2. MATERIAL AND METHODS

### 2.1 FSI framework

FSI generally uses 1-way or 2-way modelling approach. In the 1-way approach, a converged solution is obtained for one field then used as a boundary condition for the second field. On the other hand, the 2-

way approach solves fluid and solid equations separately and iterates within each time step to obtain an implicit solution. Implicit means the dependencies between the fluid and solid fields are converged within a time step. 1-way FSI are easier to implement compared to 2-way FSI due to uncertainties of obtaining convergence and the potential of having numerical singularities during the simulation in the interface and fluid domain [14]. Applications with weak physical coupling wherein the primary objective is to obtain maximum structural stresses and with strains not significant enough to affect the CFD results are most suitable for a 1-way FSI. The modelling approach used in this paper is a 1-way FSI analysis utilising a standard  $\kappa$ - $\epsilon$  turbulence model. The 1-way FSI methodology flowchart used in this study is described in Fig 1. The assumptions for the steady state simulation comprised a three-dimensional, fully-turbulent, and incompressible flow. The turbulent nature of the flow was modelled by the standard  $\kappa$ - $\epsilon$  model. The CFD code used the Finite Volume Method (FVM) approach and employed the Semi-Implicit Method for Pressure-Linked Equations (SIMPLE) velocity-pressure coupling algorithm with the second order upwind discretisation. The simulations were completed using parallel processing on a workstation with two Intel Xeon 2.0 GHz processor and 64GB Fully-buffered DDR2.

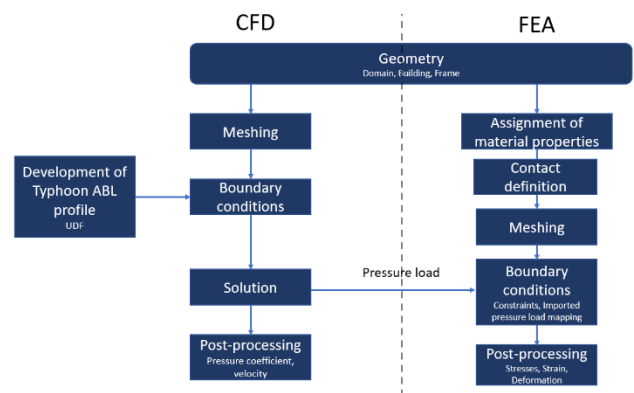


Figure 1. Proposed Fluid-Structure Interaction (FSI) framework for buildings

### 2.2 Computational domain and boundary conditions

The CFD and FEA geometry which consists of the building model (frame and sheathing) and micro-climate computational domain were constructed using the commercial CAD software Solidworks. Solidworks allowed the different components of the building to be created and combined into a 3D assembly. The integration of Solidworks with ANSYS enabled a seamless and more efficient workflow preventing the creation of

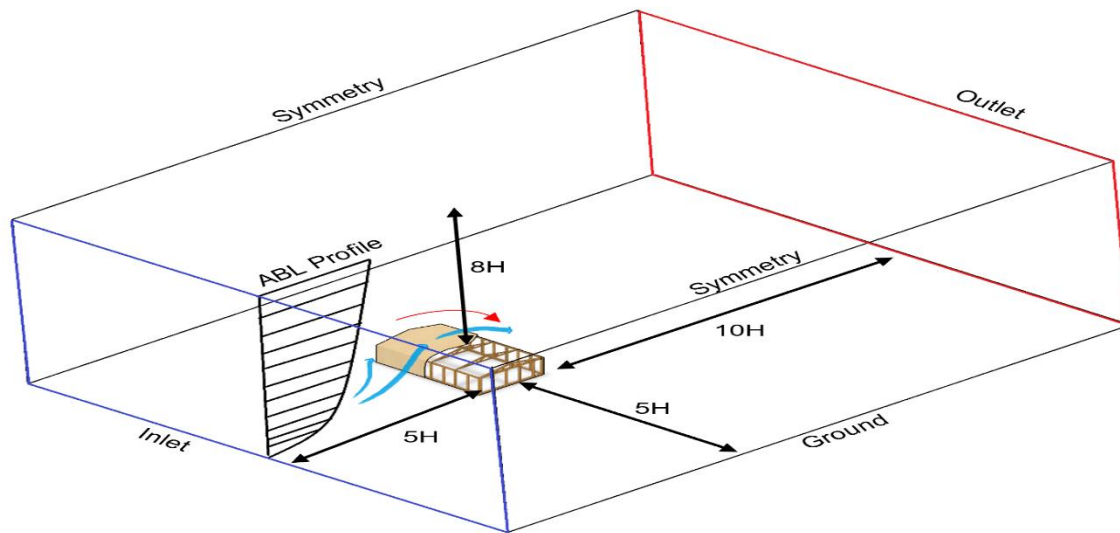


Figure 2. Computational domain and boundary conditions for the simulation of the low-rise building

several different CAD model iterations within Solidworks when modifying dimensions and iterating through designs. The benchmark building model used in the simulation is a gabled-roof building with a roof pitch of 14 degree. This gabled roof design is typical in the Philippines particularly low-rise housing [8]. The size of the computational domain which is 57 m x 38 m x 27 m as described in Figure 2 complies with the guidelines recommended in best practice guidelines [9] for directional blockage ratio. The dimension of the building is 11.78 m x 7.56 m x 3 m (L x W x H). The solar panels which has dimensions of 1.559 m x 1.046 m x 0.046 m (L x W x H) were modelled after a commercial Sunpower 310W solar panel which is constructed using an anodised aluminium 6063 frame and high transmission tempered glass. The approach profiles for the airflow velocity  $U$  and turbulent kinetic energy (TKE) are imposed at the inlet, with the stream-wise velocity of the incident airflow following a modified power law with an exponent equal to 0.077 (power law) which was generated by Song et al [10] specifically for typhoons. The velocities used were 40.68 m/s (147 kph) and 61 m/s (220 kph) at a height of 10 m. categories. A non-uniform polyhedron mesh was employed in the volume and surfaces of the computational domain. The global mesh was set to medium with smoothing set to high. Face sizing with element sizing of 50 mm was applied to the surfaces of the house. Inflation was applied to the house and ground with both having maximum layers of 5 and growth rate of 1.2. The polyhedron mesh was automatically generated from FLUENT in which all tetrahedron

elements were converted into polyhedron elements which resulted into a total of 1825345 elements. The rationale for the adaptation of the polyhedron mesh is the reduction of the number of elements without compromising accuracy.

### 2.3 Structural model components

The building as shown in Figure 3 is modelled by using the ANSYS Mechanical tool, and the structure components are represented directly by the built-in elements in ANSYS. The structure is composed of frames from SPF and sheathing panels made from 7/16 in. (12.7 mm) Oriented Strand Board (OSB) in which the material properties derived from literature [11] are incorporated in the FEA model. The OSB sheathing panels has a modulus of elasticity of 5100 MPa for E1, 15900 MPa for E2, 1590 MPa for E3, shear modulus of 790 MPa, Poisson's ratio of 0.08 and density 600 kg/m<sup>3</sup>. Three different sizes of beams were used: double 2 x 3 (63.5 x 76.2 mm) for the wall top plate, triple 2 x 3 (76.2 x 76.2 mm) for the corner walls and single 2 x 3 (38.1 x 63.5 mm) for all other frames. The 2 x 3 SPF has a modulus of elasticity of 8274MPa, shear modulus of 2955MPa and Poisson's ratio of 0.4. Thirty six solar panels were installed to cover the entire roof area. These panels are evenly spaced apart with the minimum distance of 100 mm from the roof edges. The panels were modelled as an assembly composed of anodised aluminium 6063 and high transmission tempered glass (front glass) in which the material properties also obtained from literature. The other parts of the panel such as monocrystalline solar cells and junction box were

not included to simplify the model and because they are not structurally integral parts.

### 2.4 Structural model meshing and boundary conditions

The boundary conditions for the structural model are to be set independently from the CFD analysis. The CFD domain will be suppressed in the setup and the appropriate material to be assigned in the sheathing,

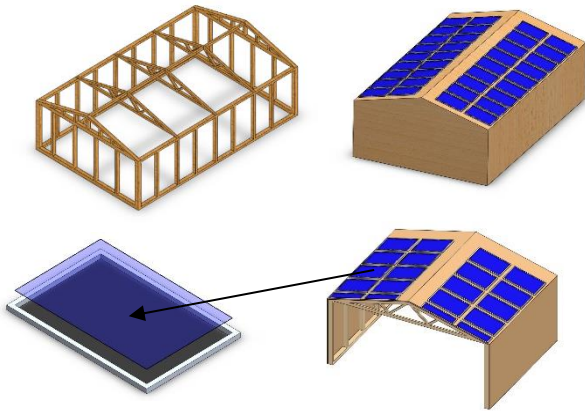


Figure 3. 3D model of frame and sheathing with 36 solar panels

frame, tempered glass and aluminium frame. Contact behaviour in this case is a no separation type of contact were assigned in the sheathing areas to the corresponding frame members which is enough already for this study. The tempered glass edges were bonded to the frame in which the frame was attached to the roof sheathing. There is also a potential towards the use of more modelling of connections particularly nail behaviour to further improve accuracy. A fixed support constraint was applied in the base of the frame and a standard earth gravity load was also added to correspond to the weight of the structure. The pressure data from the completed CFD analysis was added as an imported load. The process to interpolate the pressure data took 12 hours to finish. The FEA mesh which is separate from the CFD mesh generated an unstructured tetrahedron mesh with 1258135 elements. The body sizing method was applied for similar sizing with the CFD elements for the frame and the sheathing.

## 3. RESULTS AND DISCUSSION

Following the validated FSI methodology, building was subjected to wind speeds of  $U_{10} = 40.68\text{m/s}$  and  $U_{11} = 61\text{ m/s}$  at 0 degree and 90 degree wind angles at the same boundary conditions to investigate the air flow and pressure fields around building models. Furthermore, this will also test the structural performance of the solar panels and other building components. The wind direction angles and solar panel arrangements are shown in Figure 4. The succeeding sections describes the fluid dynamics results such as flow field velocity and surface pressure coefficient followed by structural response (equivalent stress, deflection) findings using FEA.

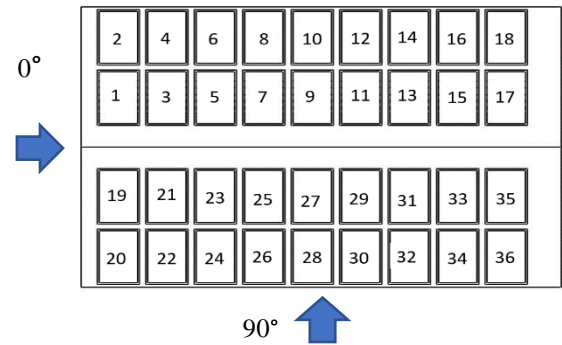


Figure 4. Wind direction angles and solar panel arrangements with labels

### 3.1 Flow velocity and pressure

Figure 5 shows the velocity contours of a cross sectional plane at 0 degree wind direction angle subjected at both wind speeds while Figure 6 shows the velocity contours at a 90 degree wind direction angle. As observed, there is a significant change in the flow fields between the 0 degree and 90 degrees wind angle direction. A weak velocity or recirculation region is observed on the roof on the 90 degrees wind angle direction due to flow separation while recirculation occurred at the 0 degree wind angle direction. The positive pressure in front of the building is greater in the 0 degree wind angle. A negative peak pressure can be observed for the windward corner ridges at both wind directions and minimal for the leeward ridge. Higher negative peak pressures are observed in the windward ridge of the 90 degree wind angle direction.

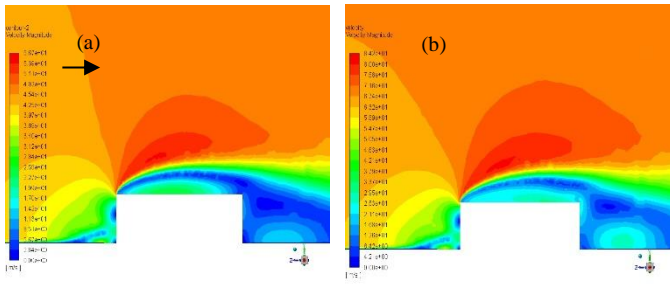


Figure 5. Velocity contours at 0° wind direction (a)  $U_{10} = 40.68\text{m/s}$  and (b)  $U_{11} = 61\text{ m/s}$

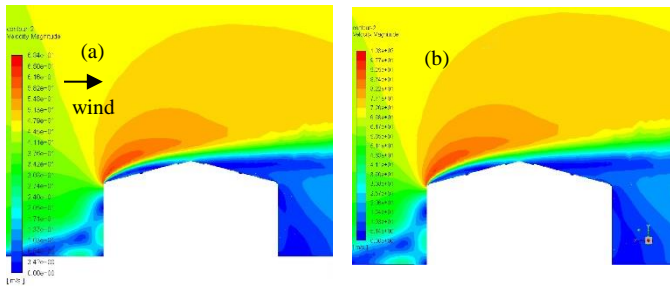


Figure 6. Velocity contours at 90° wind direction (a)  $U_{10} = 40.68\text{m/s}$  and (b)  $U_{11} = 61\text{ m/s}$

### 3.2 Panel and roof sheathing

Figures 7 and 8 shows the deformation results on both the building and panels at both wind angles. Based on the results, the highest deformation in the panels occurs at the centre of the panel itself. This is due to the uplift forces caused by the negative pressure. The highest displacement also occurs at the windward side of the roof on both scenarios and the deflection is much more- less for the panels in the leeward edge. Furthermore, the panels are less affected with lower displacements as they move away from the windward edge. The 90 degree wind angle direction had higher panel deflections (Fig. 8) than the panels oriented in the 0 degree wind angle direction (Fig. 7). This is due to higher negative pressures in the windward edge at the 90 degree wind angle orientation. Lastly, the higher wind speed resulted into a significant increase in panel deflections with the worst- case scenario at 43 mm displacement of panel no. 30 at the 90 degree orientation. Roof sheathing displacement was also observed in all results with deflections less significant compared to the panel displacements

Figure 7. Displacement contours at 0° wind direction (a)  $U_{10} = 40.68\text{m/s}$  and (b)  $U_{11} = 61\text{ m/s}$

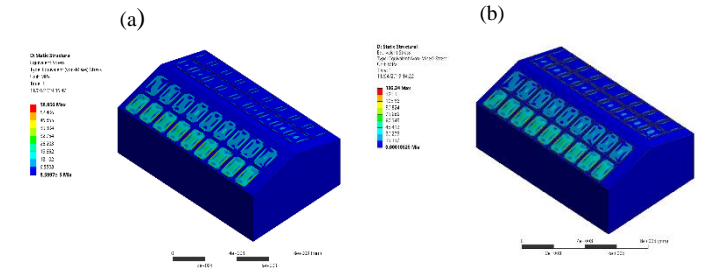


Figure 8. Displacement contours at 90° wind direction (a)  $U_{10} = 40.68\text{m/s}$  and (b)  $U_{11} = 61\text{ m/s}$

### 3.3 Panel stresses

The maximum stress induced in the panels are located on the edges of the tempered glass at the interface of the frame. This was observed in all cases. As observed in the previous section, the panel will have a high deflection in the middle resulting into high stress concentration along its edges. This panel would most likely to fail or break in this area. Minimal stresses were also experienced by the frame. Figure 9 and 10 shows the equivalent stress distribution on both wind angle orientations at two different wind speeds. Per visual inspection of the results, higher stress is observed for panels located in the windward side of the roof. The stress is significantly higher at the 61 m/s wind speed and at the 90 degree wind angle direction which exhibited the highest equivalent stress experienced by a panel at 136 MPa. Panels which are further away from the windward edge experience less amount of stress compared to the panels closer to the edge. This is the same observation made in the displacement results since higher deflections would also yield higher stresses. It was also observed that panels located closer to the windward edge tend to have higher stresses compared to the panels that are further away from that edge.

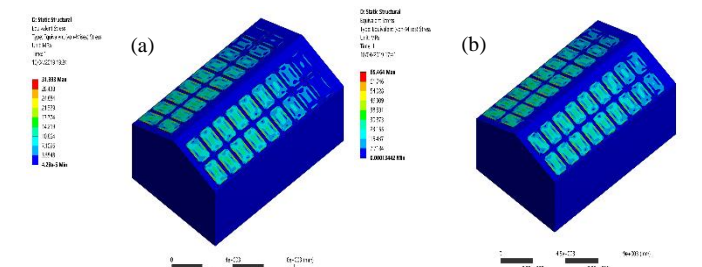
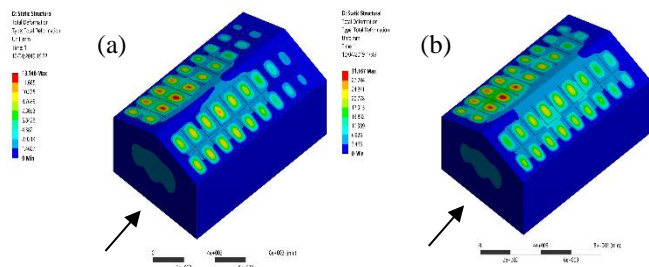


Figure 9. Equivalent stress at 0° wind direction (a)  $U_{10} = 40.68\text{m/s}$  and (b)  $U_{11} = 61\text{ m/s}$

## REFERENCE

[1] Evans A. Annual Tropical Cyclone Report 2013. Pearl Harbor, Hawaii: Joint Typhoon Warning Center; 2014.

[2] NEDA. Final Report Re Effects of Typhoon “Yolanda” (Haiyan). In: National, Council DRRaM, editors. Quezon City, Philippines; 2014.

[3] NEDA. Reconstruction Assistance for Yolanda. In: National, Authority EaD, editors. Pasig City, Philippines; 2013.

[4] Chen SE, Leeman ME, English BJ, Kennedy AB, Masters FJ, Pinelli JP, et al. Basic Structure System Rating of Post-Super Typhoon Haiyan Structures in Tacloban and East Guiuan, Philippines. *Journal of Performance of Constructed Facilities*. 2016;30(5):11.

[5] Ranada P. Architects to design storm-ready homes for Visayas Manila 2013 [Available] from: <https://www.rappler.com/move-ph/issues/disasters/typhoon-yolanda/44272-ph-architects-design-homes-haiyan>.

[6] Enteria N. CFD Evaluation of Philippine Detached Structure with Different Roofing Designs. *Infrastructures*. 2016;1(1):3.

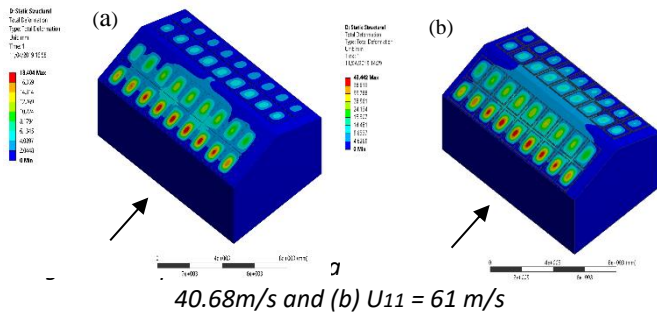
[7] Aly A, Chokwittaya C, Poche, R. Retrofitting building roofs with aerodynamic features and solar panels to reduce hurricane damage and enhance eco-friendly energy production. *Sustainable Cities and Society*. 2017; 35: 581-594.

[8] Enteria N, Awbi H, Yoshino H. Application of renewable energy sources and new building technologies for the Philippine single family detached house. *International Journal of Energy and Environmental Engineering*. 2015;6(3):267-94.

[9] Blocken B. Computational Fluid Dynamics for urban physics: Importance, scales, possibilities, limitations and ten tips and tricks towards accurate and reliable simulations. *Building and Environment*. 2015;91:219-45

[10] Song, L. L., Chen, W. C., Wang, B. L., ZHI, S. Q. & LIU, A. J. Characteristics of wind profiles in the landfalling typhoon boundary layer. *Journal of Wind Engineering and Industrial Aerodynamics*, 2016; 149, 77-88.

[11] He J, Pan F, Cai CS, Habte F, Chowdhury A. Finite-element modeling framework for predicting realistic responses of light-frame low-rise buildings under wind loads. *Engineering Structures*. 2018;164:53-69.



## 4. CONCLUSION

The study has successfully demonstrated the capability of the proposed FSI methodology for the analysis of a low rise timber frame building with solar panel installations aerodynamic-structural performance under typhoon winds. A three-dimensional structural model of the building, roofing support and solar panel assembly was developed, and the structural analysis performed using FSI to predict displacement and stress of the solar panel frame and tempered glass. Based on the results, the area of the highest uplift is found to be at the 90-degree wind angle which incurred the highest stress concentration and the maximum deformation in the solar panels. The importance of the wind angle can play the importance role in the orientation of houses. It was also determined that the solar panel's tempered glass is significantly affected during the course of a super typhoon. Panels should be located as far away as possible from the edge to minimise damage as seen from the results. Damage to the panels was also observed to be less in the leeward side of the roof. Using the proposed methods, engineers and builders can properly position renewable energy installations to minimise damage during typhoons. Optimisation studies can also be further utilised following this FSI methodology considering parameters such as roof shape, solar panel positions, wind direction and materials. Future directions of this study can include the evaluation of different roofing designs with solar panel installations such as gabled with eaves overhang, mono-sloped, domed and hip. With regards to the modelling approach, more advanced approaches such as FSI two way coupling and the use of FEA non-linear analysis will be considered to further increase the accuracy.

## ACKNOWLEDGEMENT

The authors would like to acknowledge the support by the Department of Science and Technology's (DOST-SEI)